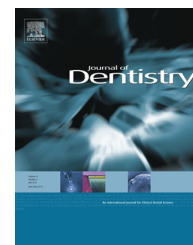


Available online at www.sciencedirect.com

ScienceDirect

journal homepage: www.intl.elsevierhealth.com/journals/jden

Effect of layered double hydroxide intercalated with fluoride ions on the physical, biological and release properties of a dental composite resin

Loredana Tammaro^{a,*}, Vittoria Vittoria^a, Anna Calarco^{b,d},
Orsolina Petillo^{b,d}, Francesco Riccitiello^c, Gianfranco Peluso^{b,d}

^a Department of Industrial Engineering, University of Salerno, Fisciano, SA, Italy

^b Institute of Protein Biochemistry, CNR, Naples, Italy

^c Conservative Odontostomatology and Maxillofacial Surgery, University of Naples, Naples, Italy

^d Institute of Biosciences and BioResources, CNR, Naples, Italy

ARTICLE INFO

Article history:

Received 9 July 2013

Received in revised form

30 October 2013

Accepted 31 October 2013

Keywords:

Dental materials

Composite resin

Layered double hydroxide

Fluoride release

Cell proliferation

ABSTRACT

Objectives: The aim of this work was the preparation of a new fluoride-releasing dental material characterized by a release of fluoride relatively constant over time without any initial toxic burst effect. This type of delivery is obtained by a matrix controlled elution and elicits the beneficial effect of a low amount of fluoride on human dental pulp stem cells (hDPSCs) towards mature phenotype.

Methods: The modified hydrotalcite intercalated with fluoride ions (LDH-F), used as filler, was prepared via ion exchange procedure and characterized by X-ray diffraction and FT-IR spectroscopy. The LDH-F inorganic particles (0.7, 5, 10, 20 wt.%) were mixed with a photo-activated Bis-GMA/TEGDMA (45/55 wt/wt) matrix and novel visible-light cured composites were prepared. The dynamic thermo-mechanical properties were determined by dynamic mechanical analyzer. The release of fluoride ions in physiological solution was determined using a ionometer. Total DNA content was measured by a PicoGreen dsDNA quantification kit to assess the proliferation rate of hDPSCs. Alkaline phosphatase activity (ALP) was measured in presence of fluoride resins.

Results: Incorporation of even small mass fractions (e.g. 0.7 and 5 wt.%) of the fluoride LDH in Bis-GMA/TEGDMA dental resin significantly improved the mechanical properties of the pristine resin, in particular at 37 °C. The observed reinforcement increases on increasing the filler concentration. The release of fluoride ions resulted very slow, lasting months. ALP activity gradually increased for 28 days in hDPSCs cell grown, demonstrating that low concentrations of fluoride contributed to the cell differentiation.

Conclusions: The prepared composites containing different amount of hydrotalcite filler showed improved mechanical properties, slow fluoride release and promoted hDPSCs cell proliferation and cell differentiation.

© 2013 Elsevier Ltd. All rights reserved.

* Corresponding author at: Department of Industrial Engineering, University of Salerno, Via Giovanni Paolo II, 132, 84084 Fisciano, SA, Italy. Tel.: +39 089 96 4019; fax: +39 089 96 4057.

E-mail address: ltammaro@unisa.it (L. Tammaro).

0300-5712/\$ – see front matter © 2013 Elsevier Ltd. All rights reserved.

<http://dx.doi.org/10.1016/j.jdent.2013.10.019>

1. Introduction

The rapid increase of interest in the field of bio-hybrid materials that exhibit improved structural and functional properties is more and more attracting researchers from life science, materials science, and nanoscience. Concomitant results offer valuable opportunities for applications that involve disciplines dealing with engineering, biotechnology, medicine and pharmacy, agriculture, nanotechnology, and others.

Nano-structured modification of both thermoplastic and thermosetting polymers, using inorganic fillers dispersed at nanoscale, has opened up new perspectives for multifunctional materials. By choosing the appropriate synthetic polymer or resin as well as the specific fillers, unprecedented morphological control down to the nanoscale is obtained. The potential for new multifunctional materials lies in the versatility of both the polymer and the inorganic chemistry that can be exploited in the materials synthesis.^{1–7}

Great attention has recently emerged around the composites in which layered fillers are dispersed at a nanometric level in a polymeric matrix. Such composites possess unusual properties, very different from their microscale counterparts. In particular Layered Double Hydroxide (LDHs), or hydroxide-like compounds, have attracted considerable attention in the recent decade for their applications in many fields.^{8–11} LDHs consist of flat two-dimensional network composed of different hydroxy layers of bivalent and trivalent metal ions. Isomorphic substitution of some bivalent metal ions of LDHs with trivalent ions gives rise to positive residual charges in the framework which is counterbalanced with anions and water molecules located interstitially. These compounds, also known as “anionic clays”, have the general formula $[M(II)_{(1-x)}M(III)_x(OH)_2](A_{x/n})_mH_2O]$, where M(II) is a divalent cation such as Mg, Ni, Zn, Cu or Co and M(III) is a trivalent cation such as Al, Cr, Fe or Ga with A^{n-} an anion of charge n such as $(CO_3)^{2-}$, Cl^- , NO_3^- or organic anion.

One of the still open problems in polymer resins for dental applications is the micro leakage between the sealant and tooth surface causing bacterial invasion and secondary caries. Several types of resin, both filled and unfilled, have been employed as a pit and fissure sealants.¹² Over the years, several researches have been conducted on sealant materials and methods to improve their properties like retention, marginal integrity, etc., but today there is a need of materials for remineralization. Calcium and phosphate ions from saliva or other sources (dentifrices, chewing gums, beverages, remineralizing solutions and restorative materials), and fluoride from topical or systemic sources, have the potential to re-mineralize the carious lesions or minimize caries development.

The anti-cariogenic property of the fluoride is well documented and involves various mechanisms including the reduction of the demineralization, the enhancement of the remineralization, the interference of pellicle and plaque formation and the inhibition of microbial growth and metabolism.^{13–20}

The beneficial effects of the fluoride arise from its incorporation in tooth mineral as fluoroapatite leading to the decreased solubility of the tooth enamel.²¹

In addition, fluoride can affect dentinogenesis through the modulation of proliferation and differentiation of Dental Pulp Stem Cells (DPSCs), self-renewable multipotent stromal cells of the pulp, fundamental for dental tissue regeneration. However, this last effect of fluoride is dose-dependent. Only low concentrations of fluoride can positively affect the differentiation of normal human DPSCs (hDPSCs) *in vitro*, while high fluoride concentration has inhibitory effects on the same cells.²²

This cell biological response to different fluoride amounts is of importance to thoroughly investigate the influence of fluoride-releasing restorative dental materials (F-RM) on pulp stem cells.

Indeed, the first attempts to produce F-RM, which could act as a fluoride reservoir increasing the fluoride level in saliva, plaque and dental hard tissues, were prompted by the concept that fluoride-release from the materials exerted useful effects in the clinical practice reducing the incidence of dental caries not only by inhibiting microbial growth, but also improving tooth regeneration and reconstruction capacity.

But recently, it was demonstrated that F-RM could be toxic for hDPSCs and that the differences in cytotoxicity between the tested F-RM were related to the amount of fluoride released.^{23–25} It appears, therefore, that it should pay more attention to improve F-RM characteristics in an attempt to control the release of fluoride avoiding, in particular, the initial burst release characterized by high, potentially toxic, fluoride concentrations.

Release of fluoride is under the influence of some internal variables such as material formulation, filler, and fluoride content.

In this paper we present the formulation, preparation and characterization of novel visible-light cured composites based on photo-activated Bis-GMA/TEGDMA matrix, containing a filler based on an hydroxide-like compound intercalated with fluoride ions. We have obtained a dental resin with improved physical and biological properties and, in addition, able to release low amount of fluoride in a controlled and tunable way for a long period of time.

In contrast to the conventional and resin-modified glass-ionomers, our F-RM show to have no initial toxic fluoride ‘burst’ effect and levels of fluoride release remain relatively constant over time. This type of delivery is obtained by a matrix-controlled elution and elicits the beneficial effects of low amount of fluoride on hDPSC differentiation.

This study represents a first successful attempt to prepare a fluoride-releasing material based on a commercial dental resin. A forthcoming paper will deal with the degree of conversion and polymerization shrinkage of the prepared composite resins.

2. Materials and methods

2.1. Preparation of fluoride layered double hydroxide (LDH-F)

The intercalation of the fluoride anions in the LDH was performed by equilibrating, at room temperature, under stirring and under nitrogen flow for 48 h, 500 mg of LDH in

the nitrate form $[\text{Mg}_{0.65}\text{Al}_{0.35}(\text{OH})_2](\text{NO}_3)_{0.35} \cdot 0.68\text{H}_2\text{O}$ (LDH- NO_3), with 10 ml of a CO_2 -free aqueous solution 0.25 mol/dm³ of fluoride sodium salt, NaF, (F^-/NO_3^- molar ratio = 1.3).^{26,27} The obtained white solid was separated by centrifugation, washed three times with CO_2 -free deionized water and finally dried at rt over a saturated NaCl solution (75% of relative humidity, RH). The final product (sample LDH-F) has the formula $[\text{Mg}_{0.65}\text{Al}_{0.35}(\text{OH})_2](\text{F})_{0.35} \cdot 0.8\text{H}_2\text{O}$.

2.2. Dispersion of LDH-F into dental matrix

The LDH-F (with mass fraction of 0.7, 5, 10 and 20%) was added into a commercial light-activated restorative material (RK) provided by Kerr s.r.l. (Italy), which consisted of bisphenol-A glycidyl dimethacrylate (Bis-GMA), tri-ethylene glycol dimethacrylate (TEGDMA), camphorquinone (CQ), ethoxylated bisphenol A dimethacrylate (EBPADMA) and glass fillers. Specimen disks 20 mm in diameter and 1 mm thick, were fabricated using steel molds. The composite obtained were then cured by photo-polymerization using a visible light curing unit (Optilux 380, distributed through KERR, USA; irradiated diameter: 11 mm) with an irradiation time of 120 s. During the experiment, the light intensity was maintained at 550 mW/cm². The samples are coded RK-Fx, where x is the percentage by weight of the inorganic solid LDH-F in the resin RK.

2.3. Characterization and evaluation

2.3.1. X-ray powder diffraction (XRPD)

XRPD patterns were recorded, in reflection, with an automatic Bruker diffractometer (equipped with a continuous scan attachment and a proportional counter), using the nickel filtered $\text{Cu K}\alpha$ radiation ($\lambda = 1.54050 \text{ \AA}$) and operating at 40 kV and 40 mA, step scan 0.05° of 2θ and 3 s of counting time.

2.3.2. Fourier transform infrared analysis (FT-IR)

Infrared absorption spectra were obtained by a Bruker spectrophotometer, model Vertex 70, with a resolution of 4 cm^{-1} (32 scans collected).

2.3.3. Dynamic-mechanical analysis

Dynamic-mechanical properties of the samples were performed in triplicate with a dynamic mechanical thermo-analyzer (TA instrument-DMA 2980). The samples were tested by applying a variable flexural deformation in dual cantilever mode. The displacement amplitude was set to 0.1%, whereas the measurements were performed at the frequency of 1 Hz. The range of temperature was -50 to $150 \text{ }^\circ\text{C}$, scanning rate of $3 \text{ }^\circ\text{C}/\text{min}$.

2.3.4. Fluoride release study

Weighed disks were put in contact with a fixed volume of 50 ml of a physiological saline solution (NaCl 0.90% w/v) under stirring at $37 \text{ }^\circ\text{C}$. After specific time intervals (after an hour for the first six hours, then every 12 h) the measurement of the fluoride concentration (ppm) of each solution was carried out using a ionometer (Thermo Orion Mod 720 Aplus). The measurements were made in triplicate and averaged the values.

2.3.5. Primary cell culture

Human dental pulp stem cells (hDPSCs) were isolated as described previously.^{28,29} Briefly, human impacted third molars from 10 adults (18–22 years of age) were collected at Federico II University Dental Hospital (Naples, Italy). The experimental protocol was approved by the Hospital's Institutional Review Board (accession number 7413), and the patients provided informed consent. The teeth were cracked open to remove the pulp tissues gently with forceps. The pulp tissues were then minced and digested in a solution of 3 mg/ml collagenase type I and 4 mg/ml dispase (Sigma-Aldrich, Italy) for 30 min at $37 \text{ }^\circ\text{C}$. The digested mixtures were passed through a 70- μm cell strainer (Falcon, Italy) to obtain single-cell suspensions. Cells were seeded onto six-well plates and cultured with α -minimum essential medium (α -MEM) supplemented with 15% FBS, 2 mM L-glutamine, 100 μM L-ascorbic acid-2-phosphate, 100 U/ml penicillin-G, 100 $\mu\text{g}/\text{ml}$ streptomycin, and 0.25 $\mu\text{g}/\text{ml}$ fungizone (Hyclone, Italy) and maintained in 5% CO_2 at $37 \text{ }^\circ\text{C}$. Colony formation units of fibroblastic cells were normally observed within 1–2 weeks after cell seeding and were passaged at 1:3 ratio when they reached ~80% confluence changing medium every 2 days. Heterogeneous populations of hDPSCs were frozen and stored in liquid nitrogen at passages 0–2. Before incubation with cells, all the RK-Fx resins were gas sterilized using ethylene oxide. Second passage hDPSCs were seeded at a concentration of 1×10^4 cells/well directly onto RK-Fx resins (14 mm in diameter) placed in 24-well plates (Falcon). The non-adherent cells were removed by washing three times in medium at 24 h.

2.3.6. hDPSC proliferation assay

To assess the proliferation rate of the cells, total DNA content ($n = 3$) was measured by a PicoGreen dsDNA quantification kit (Molecular Probes, Italy). Cells were seeded at a density of 4×10^3 cells/well in a 96-well plate, and after 24-h incubation, medium was replaced with fluoride-medium (fluoride final concentrations of 0.5, 1.0, 2.0 and 5.0 ppm) for a further 48 h. Then cells were washed twice with a sterile phosphate buffer saline (PBS) solution and transferred into 1.5-ml microtubes containing 1 ml of ultrapure water (Eppendorf, Italy). Samples were incubated for 1 h at $37 \text{ }^\circ\text{C}$ in a water bath, subjected to a freeze-thaw cycle and sonicated for 15 min before DNA quantification. Then 100 μl of PicoGreen working solution was added to 100 μl of supernatants of the samples. Triplicates were made for each sample or standard. The plate was incubated for 10 min in the dark and fluorescence was measured on a microplate reader (Fluostar Optima, BMG Lab technologies) using an excitation wavelength of 490 nm and an emission of 520 nm. A standard curve was created and sample DNA values were read off from the standard graph.

2.3.7. Alkaline phosphatase activity

Alkaline phosphatase activity is a typical marker for early odontoblastic differentiation. To examine whether the fluoride release by the different resins-induced ALP activity in hDPSCs, ALP activity was assessed as reported by Wang et al.³⁰ Briefly, hDPSCs were cultured on RK-Fx disks (RK-F0.7 and RK-F10, 14 mm diameter) for 1, 7, 14 and 28 days. Then, the cells were scraped into cold PBS, sonicated in an ice bath and centrifuged at $1500 \times g$ for 15 min. ALP activity was measured

in the supernatant using p-nitrophenyl phosphate as a phosphatase substrate and alkaline phosphatase supplied by the kit as a standard. The absorbance was measured at 405 nm and the amount of ALP in the cells was normalized against total protein content.

2.3.8. Assessment of extracellular matrix mineralization

hDPSC cells were seeded on fluoride-releasing resins (RK-F0.7 and RK-F10) at a density of 1×10^5 cells/well and cultured for 14 days. Calcified extracellular matrix (ECM) was observed by alizarin red S staining (Sigma–Aldrich). After culture, the wells were washed three times with PBS (pH 7.4) and fixed in a 4% para formaldehyde solution for 20 min. Cells were stained with a 20 mg/ml alizarin red S solution in 0.1% NH_4OH at pH 4.2 for 20 min at room temperature. To quantify matrix mineralization, alizarin red S was solubilized in 100 mmol/l cetylpyridinium chloride for 1 h, and the absorbance of the solution was measured at 570 nm. Mean absorbance values were obtained from 3 independent experiments.

2.4. Statistical analysis

All data were reported as mean with standard deviation ($n = 3$). Statistical analysis was evaluated by a Student's t-test for differences among groups and a value of $P < 0.05$ was considered statistically significant.

3. Results and discussion

3.1. Structural analysis of fluoride hydrotalcite (LDH-F)

Structural information was obtained by X-ray analysis (XRPD) and FT-IR absorption spectroscopy. Fig. 1(a) shows the diffraction patterns of the pristine hydrotalcite in nitrate form (LDH- NO_3) and the intercalated fluoride form (LDH-F). As a result of the NO_3/F exchange, the X-ray reflection due to the interlayer distance ($d_{003} = 0.902$ nm) and positioned at $2\theta = 9.9^\circ$ (LDH- NO_3) moves at much higher angles, $2\theta = 11.68^\circ$, corresponding to an interlayer distance of 0.757 nm (LDH-F). The decrease of the interlayer distance was due to the intercalation of the fluoride anion with smaller dimension than the nitrate

anion.³¹ The second and third patterns of LDH-F spectra correspond to the higher harmonics of the interlayer distance. All the peaks are sharp, and this indicates an ordered accommodation of the inorganic anion within the interlayer regions. Moreover, the X-ray reflections of the nitrate form are absent, and this indicates that the nitrate ions left out of the exchange were solubilized in the interlayer region of the fluoride intercalate.

Fig. 1(b) shows the FT-IR absorbance spectra for the LDH-F sample. The intercalation of fluoride ions into LDH is represented by the characteristic band at frequency 1385 cm^{-1} .^{31,32} Adsorption bands around 550 and 680 cm^{-1} can be attributed to the Mg–OH and Al–OH translation modes, respectively.³³ The adsorption band around 3460 cm^{-1} can be attributed to the OH group stretching due to the presence of hydroxyl groups of LDH, co-intercalated water molecules, or both.³⁴

3.2. Incorporation of LDH-F into the dental resin

3.2.1. Structural investigation

The incorporation and dispersion of the inorganic solid into the dental resin was investigated by X-ray analysis. The diffractograms of the LDH-F, the pure resin and the composites with LDH-F are displayed in Fig. 2. The broad pattern in Fig. 2(b) is attributed to the reflection of amorphous RK, while the diffraction spectra of RK/LDH-F composites (Fig. 2(c)–(f)) show characteristic reflections of LDH-F powders at $2\theta = 11.68^\circ$ and 23.6° besides the broad reflection of pristine RK, increasingly evident starting from the sample at 5% of concentration (RK-F5). In particular the basal peak at 11.68° of 2θ is absent at low concentration; it appears in the sample RK-F5 and then increases on increasing the inorganic concentration. This suggests that the clay is delaminated and well dispersed up to 5% of concentration, whereas at higher concentrations large clay tactoids are present in the sample. The X-ray data therefore indicate a morphology with micro-domains of LDH-F at concentrations higher than 5%.

3.2.2. Mechanical properties

The mechanical properties were investigated in a wide range of temperatures by performing a dynamic mechanical analy-

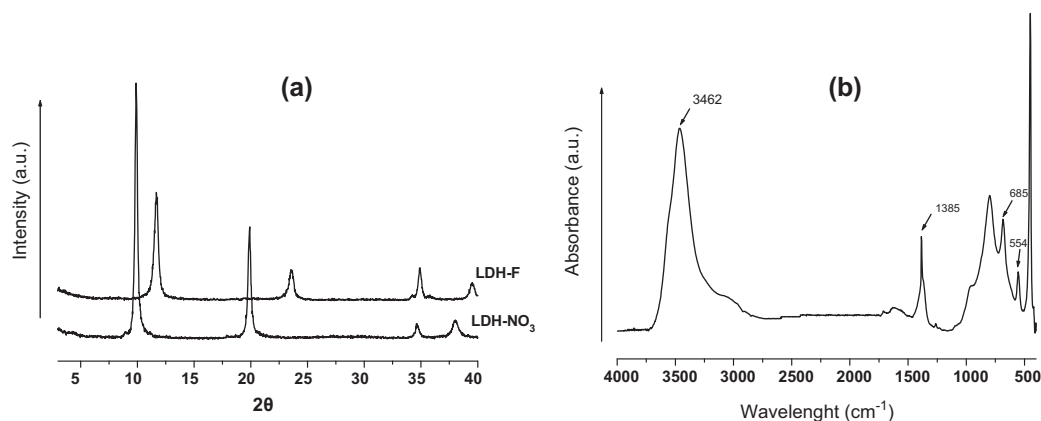


Fig. 1 – (a): XRD patterns of LDH- NO_3 and LDH-F, (b): FT-IR spectra of LDH-F.

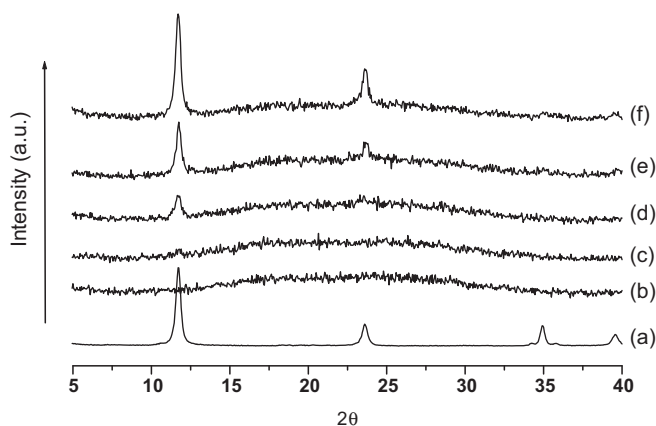


Fig. 2 – XRD patterns of: LDH-F (a), RK resin (b), RK-F0.7 (c), RK-F5 (d), RK-F10 (e) and RK-F20 (f).

sis, able to detect either the elastic modulus and the $\tan \delta$ in the investigated range of temperature. Fig. 3 shows the elastic modulus for the pristine resin and the resin containing 5, 10 and 20 wt.% of LDH-F. The study of the mechanical properties in a wide temperature range demonstrated that the values of the elastic modulus of the resins containing the fluoride inorganic solid (RK-Fx) increased compared with the resin RK. This increase, which was evident after the glass transition temperature, was observed at different temperatures and for different compositions.

The comparison of the storage moduli at three different temperatures (0 °C, 37 °C, 50 °C) and the values of the glass transition temperatures are reported in Fig. 4(a and b). We observed that the storage moduli of the composite resins are consistently higher than the pristine resin and the increase is particularly relevant at 37 °C, the body temperature. The observed reinforcement increases on increasing the filler concentration. As expected, as shown in many composite systems, the deformation at breaking of the composite resin

was found slightly lower than the pristine resin. However, since the stress is increasingly higher in the composites, the toughness remained almost unchanged.

3.2.3. Release properties

One of the main goal of this study, beside to improve the physical properties, is to obtain a resin able to release fluoride ions, in controlled and tuneable way according to the external environment to which the resin is exposed.

The resin was suspended in physiological saline solution and the release of the active ingredient was monitored over time.

A significant phenomenon was observed which constitutes a further advantage of the system: the anchorage of the active molecule to the inorganic lamellar compound allows slower release. This makes the system much more efficient. Fig. 5, shows the release of fluoride ions (in ppm) at different initial concentrations from the RK-F0.7, RK-F5, RK-F10 and RK-F20 samples.

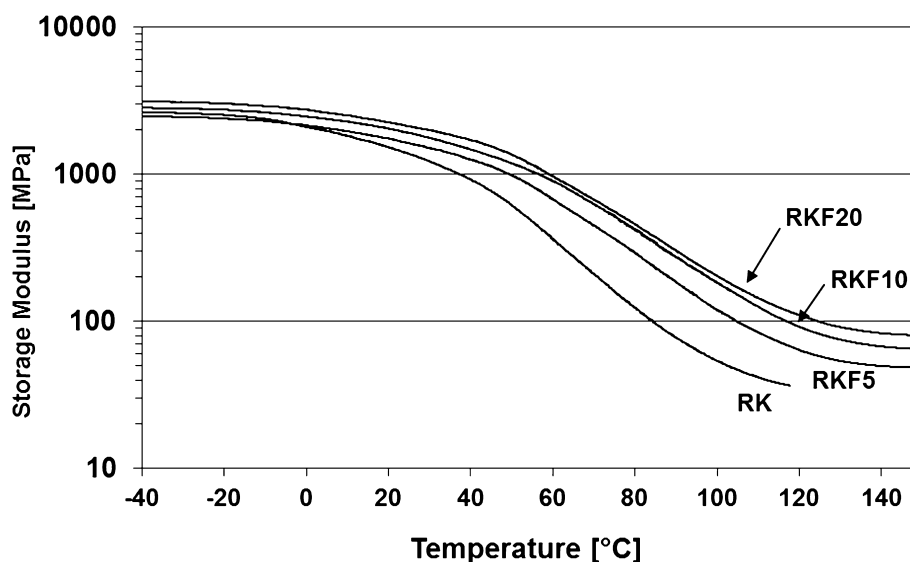


Fig. 3 – Storage modulus (MPa) versus temperature (°C) of: RK, RK-F5, RK-F10 and RK-F20.

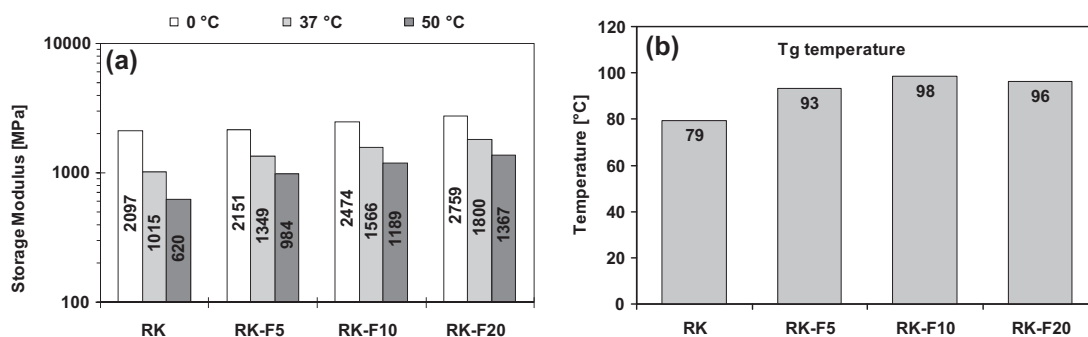


Fig. 4 – (a) Storage moduli E' (MPa) at 0 °C, 37 °C and 50 °C and (b) glass transition temperatures (°C) for the pristine resin and its composites.

We observed a rapid release at the beginning of the experiment, followed by a release linearly depending on the time (days). The first step is independent of the initial concentration, as expected for a glassy rigid polymeric matrix, in which the diffusive phenomena are only dependent on the frozen free volume. The second part of the release curve is linear with the release time. It inversely depends on concentration, in the sense that the higher the concentration the lower the released part of fluoride ions. This result reflects the strong influence of the morphology in the case of composites with lamellar clays. When the clay lamellae, where the fluoride ions are anchored, are delaminated and well dispersed in the resin, the fluoride ions, less shielded by the lamellae, are more available to be de-touched from the clay and diffuse through the resin. Increasing the clay concentration, big tactoids are formed and the fluoride ions are less available to be reached by the counter ions, detach and diffuse in the resin. Fluctuations between the different concentrations higher than 5%, are possibly due to morphology fluctuations during the composite preparation. This result indicates the possibility to have a tunable and controlled release of fluoride from RK resins.

It is worth observing that the extrapolated release can occur up to one year, with a ppm concentration released each day that is far from the possible adverse fluoride effect.

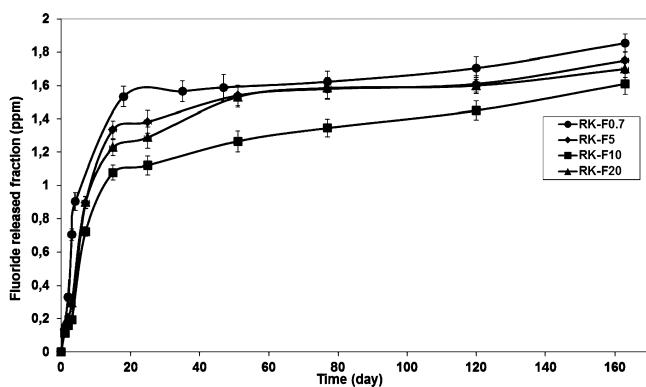


Fig. 5 – Release profiles of fluoride ions from RK-F0.7, RK-F5, RK-F10 and RK-F20 samples in physiological solution as a function of time (day).

3.2.4. Cell proliferation and ALP activity

Human DPSCs can differentiate into various tissues, such as odontoblasts, adipocytes, chondrocytes, and osteoblasts.^{28,35} In addition, hDPSCs are effective in mineralized tissue formation.^{36–38}

It has been hypothesized that the failure of dental restorations is dependent on the degree to which the pulpal cell populations can survive, as well as the ability of these cells to detect and respond to injury to initiate an appropriate repair response.^{39,40} Thus, it is fundamental to use restorative dental materials and procedures congruent with the natural regenerative activity of teeth and with the induction of odontoblast phenotype in hDPSC.

The first sparks to produce active fluoride-releasing materials, with definite interactions with the human DPSC, originated from the fact that materials capable of releasing fluoride can exert useful effects in terms of DPSC differentiation in odontoblasts. However, it has been demonstrated that the level of fluoride release was in direct correlation with cytotoxic activity of F-RM on human DPSCs, while low levels of released fluoride correlated to low cytotoxic effect on human DPSCs.⁴¹

To assess whether fluoride concentration affected the proliferation of hDPSC, we seeded growth-arrested cells (in FBS-deprived basal medium for 24 h) in 0.2% FBS and then measured cell proliferation by DNA assay using a fluorimetric dsDNA quantification kit. Fig. 6(a) demonstrated that cytotoxic concentration of fluoride was ranging between 3 and 5 ppm, a value did not present in the conditioned supernatant of fluoride release resins (RK-F0.7 and RK-F10) for all the points evaluated. Parallel experiments using the supernatants conditioned with RK-F0.7 or RK-F10 demonstrated that all the supernatants tested did not show any significant inhibition of proliferation on hDPSC. Conditioned supernatants from tissue culture polystyrene and RK were used as control (data not shown).

As showed in the previous paragraph there was no substantial difference of fluoride release from RK-F0.7 and RK-F5, so we report only the results obtained on RK-F0.7 and RK-F10.

Alkaline phosphatase activity (ALP), an early marker of odontogenic differentiation of pulp cells, was measured in cells cultured on fluoride-releasing restorative materials (RK-

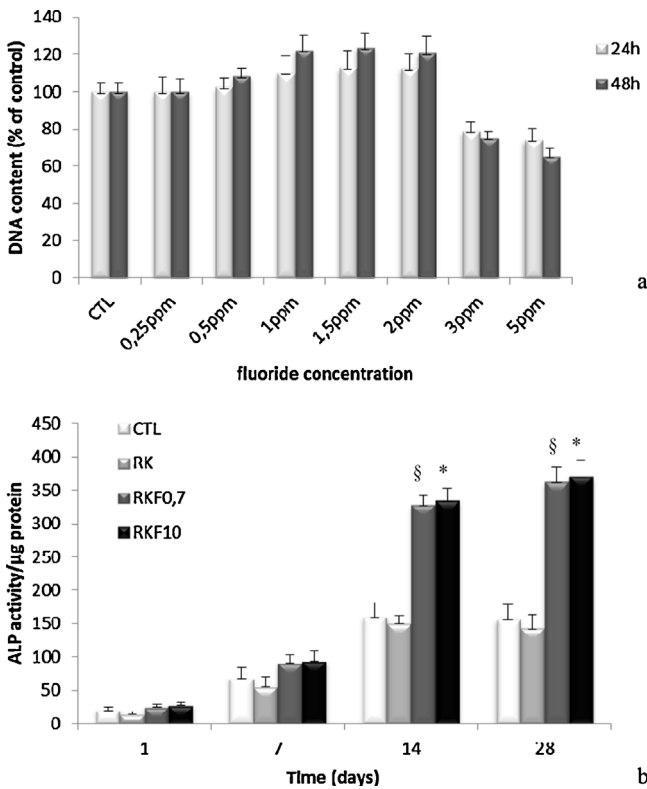


Fig. 6 – (a): Effects of fluoride concentration on hDPSCs cell proliferation after 24 and 48 h. Cell cultured onto tissue culture polystyrene were used as control (CTL). **(b)** ALP activity of hDPSCs cultured for 28 days on RK-Fs. Cell cultured onto tissue culture polystyrene (CTL) or on commercial light-activated restorative materials without fluoride (RK) were used as controls. RK-F0.7 and RK-F10 were fluoride-releasing restorative materials. The bars represent means \pm SD ($n = 3$). * $p < 0.01$ when RK-F0.7 group is compared to CTL or RK group; $^{\S}p < 0.01$ when RK-F10 group is compared to CTL or RK group.

F0.7 and RK-F10). Cells cultured on polystyrene (CTL) and on restorative material without fluoride (RK) were used as control. Fig. 6(b) shows that the ALP activity gradually increased for 28 days in cells grown on RK-F0.7 or RK-F10 compared to cells cultured onto tissue culture polystyrene and RK. Thus, the release of low amounts of fluoride from RK-F0.7 or RK-F10 was able to modulate positively hDPSCs differentiation.

3.3. Extracellular matrix mineralization

Mineralization of hDPSC was obtained via alizarin red S staining. As shown in Fig. 7, we observed no remarkable differences in calcified extracellular matrix (ECM) mineralization in cells plated on RK-F0.7 and RK-F10, as was expected based on the results of the ALP assay, compared to cells plated on RK.

These results suggest that both resins exhibit equivalent biologic activity as scaffolds supporting hDPSCs, despite different levels of fluoride released.

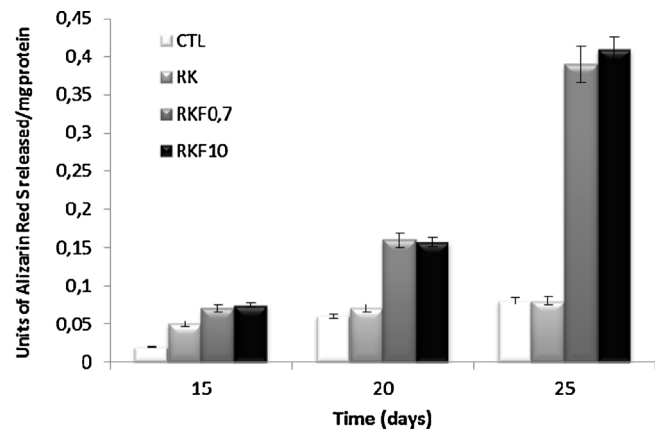


Fig. 7 – Mineralization of hDPSCs extracellular matrix on RK-Fs. At intervals during incubation on RK-Fs resins (15, 20 and 25 days), calcium deposits were measured by alizarin red S staining. Cells cultured onto tissue culture polystyrene or on commercial light-activated restorative materials without fluoride (RK) were used as controls. RK-F0.7 and RK-F10 were fluoride-releasing restorative materials. The bars represent means \pm SD ($n = 3$).

4. Conclusion

The present study investigated the effects of a modified hydroxylapatite (LDH-F) dispersed into a commercial light-activated restorative material on mechanical properties, fluoride release and hDPSCs cell proliferation. Good results make LDH-F a promising filler for dental resin.

REFERENCES

- Ruiz-Hitzky E, Darder M, Aranda P, Ariga K. Advances in biomimetic and nanostructured biohybrid materials. *Advanced Materials* 2010;22:323–36.
- Ruiz-Hitzky E, Ariga K, Lvov Y. Bio-inorganic hybrid nanomaterials. Germany: Wiley-VCH, Weinheim; 2008.
- Nejati E, Firouzdor V, Eslaminejad MB, Bagheri F. Needle-like nano hydroxyapatite/poly(L-lactide acid) composite scaffold for bone tissue engineering application. *Materials Science and Engineering C* 2009;29:942–9.
- Taguchi T, Shiraogawa M, Kishida A, Akashi M. A study on hydroxyapatite formation on/in the hydroxyl groups-bearing nonionic hydrogels. *Journal of Biomaterials Science Polymer Edition* 1999;10:19–32.
- Arimura S, et al. Hydroxyapatite formed on/in agarose gel induces activation of blood coagulation and platelets aggregation. *Journal of Biomedical Materials Research Part B Applied Biomaterials* 2007;81:456–61.
- Manzano M, Arcos D, Delgado MR, Ruiz E, Gil FJ, Vallet-Regi M. Bioactive star gels. *Chemistry of Materials* 2006;18:5696–703.
- Izquierdo Barba I, Arcos D, Sakamoto Y, Terasaki O, Lopez Noriega A, Vallet Regi M. High-performance mesoporous bioceramics mimicking bone mineralization. *Chemistry of Materials* 2008;20:3191–8.

8. Rives V. Layered double hydroxides: present and future. New York: Nova Science Publishers; 2001.
9. Choy JH, Choi SJ, Oh JM, Park T. Clay minerals and layered double hydroxides for novel biological applications. *Applied Clay Science* 2007;**36**:122–32.
10. Tammaro L, Tortora M, Vittoria V, Costantino U, Marmottini F. Methods of Preparation of novel composites of poly(ϵ -caprolactone) and a modified Mg/Al hydrotalcite. *Journal of Polymer Science Part A Polymer Chemistry* 2005;**43**:2281–90.
11. Costantino U, Bugatti V, Gorrasi G, Montanari F, Nocchetti M, Tammaro L, et al. New polymeric composites based on poly(ϵ -caprolactone) and layered double hydroxides containing antimicrobial species. *ACS Applied Materials and Interfaces* 2009;**1**:668–77.
12. Anusavice KJ. Phillips' science of dental materials. 11th ed. St. Louis, MO: Saunders; 2003.
13. Wiegand A, Buchalla W, Attin T. Review on fluoride-releasing restorative materials- fluoride release and uptake characteristics, antibacterial activity and influence on caries formation. *Dental Materials* 2007;**23**:343–62.
14. Fejerskov O, Ekstrand J, Burt BA. Fluoride in dentistry. Copenhagen: Munksgaard; 1996.
15. Ten Cate JM, Featherstone JD. Mechanistic aspects of the interactions between fluoride and dental enamel. *Critical Reviews in Oral Biology and Medicine* 1991;**2**:283–96.
16. Ten Cate JM. Current concepts on the theories of the mechanism of action of fluoride. *Acta Odontologica Scandinavica* 1999;**57**:325–9.
17. Ten Cate JM, Buijs MJ, Miller CC, Exterkate RA. Elevated fluoride products enhance remineralization of enamel. *Journal of Dental Research* 2008;**87**:943–7.
18. Gonzales-Cabezas C, Fontana M, Dunipace AJ, Li Y, Fischer GM, Proskin HM, et al. Measurement of enamel remineralization using microradiography and confocal microscopy. A correlational study. *Caries Research* 1998;**32**:385–92.
19. Schemerhorn BR, Orban JC, Wood GD, Fischer GM. Remineralization by fluoride enhanced with calcium and phosphate ingredients. *Journal of Clinical Dentistry* 1999;**10**:13–6.
20. Abudiak H, Robinson C, Duggal MS, Strafford S, Toumba KJ. Effect of fluoride sustained slow-releasing device on fluoride, phosphate and calcium levels in plaque biofilms over time measured using ion chromatography. *Journal of Dentistry* 2012;**40**:632–8.
21. Chow LC, Vogel GL. Enhancing remineralization. *Operative Dentistry* 2001;**26**:27–38.
22. Thaweboon S, Thaweboon B, Chunhabundit P, Suppukpatana P. Effect of fluoride on human dental pulp cells in vitro. *Southeast Asian Journal of Tropical Medicine and Public Health* 2003;**34**:915–8.
23. Modena K, Casas AL, Atta M, Costa C, Hebling J, Sipert C, et al. Cytotoxicity and biocompatibility of direct and indirect pulp capping materials. *Journal of Applied Oral Sciences* 2009;**17**:544–54.
24. Mount GJ. Glass-ionomer cements: past, present and future. *Operative Dentistry* 1994;**8**:2–90.
25. Chan C, Lan W, Chang M, Chen Y, Lan W, Chang H. Effects of TGF betas on the growth, collagen synthesis and collagen lattice contraction of human dental pulp fibroblasts in vitro. *Archives of Oral Biology* 2005;**50**:469–79.
26. Costantino U, Marmottini F, Nocchetti M, Vivani R. New synthetic routes to hydrotalcite-like compounds – characterisation and properties of the obtained materials. *European Journal of Inorganic Chemistry* 1998;**143**:9–46.
27. Costantino U, Ambrogi V, Nocchetti M, Perioli L. Hydrotalcite-like compounds: versatile layered hosts of molecular anions with biological activity. *Microporous and Mesoporous Materials* 2008;**107**:149–60.
28. Gronthos S, Mankani M, Brahimi J, Robey PG, Shi S. Postnatal human dental pulp stem cells (DPSCs) in vitro and in vivo. *Proceedings of the National Academy of Sciences of the United States of America* 2000;**97**:13625–30.
29. Sonoyama W, et al. Mesenchymal stem cell-mediated functional tooth regeneration in swine. *PLoS ONE* 2006;**1**:e79.
30. Wang J, Liu X, Xiaobing J, Ma H, Hu J, Ni L, et al. The odontogenic differentiation of human dental pulp stem cells on nanofibrous poly(L-lactic acid) scaffolds in vitro and in vivo. *Acta Biomaterialia* 2010;**6**:3856–63.
31. Lv L, He J, Wei M, Evans DG, Duan X. Factors influencing the removal of fluoride from aqueous solution by calcined Mg–Al–CO₃ layered double hydroxides. *Journal of Hazardous Materials* 2006;**B133**:119–28.
32. Ma W, Zhao N, Yang G, Tian L, Wang R. Removal of fluoride ions from aqueous solution by the calcination product of Mg–Al–Fe hydrotalcite-like compound. *Desalination* 2011;**268**:20–6.
33. Klopogge JT, Frost RL. Fourier transform infrared and Raman spectroscopic study of the local structure of Mg-, Ni-, and Co-hydrotalcites. *Journal of Solid State Chemistry* 1999;**146**:506–15.
34. Velu S, Amkumar V, Narayanan V, Swamy CS. Effect of interlayer anions on the physicochemical properties of zinc–aluminium hydrotalcite-like compounds. *Journal of Materials Science* 1997;**32**:957–64.
35. Iohara K, Zheng L, Ito M, Tomokiyo A, Matsushita K, Nakashima M. Side population cells isolated from porcine dental pulp tissue with self-renewal and multipotency for dentinogenesis, chondrogenesis, adipogenesis, and neurogenesis. *Stem Cells* 2006;**24**:2493–503.
36. Zhang W, Walboomers XF, van Kuppevelt TH, Daamen WF, Bian Z, Jansen JA. The performance of human dental pulp stem cells on different three dimensional scaffold materials. *Biomaterials* 2006;**27**:5658–68.
37. Wang J, Ma H, Jin X, Hu J, Liu X, Ni L, et al. The effect of scaffold architecture on odontogenic differentiation of human dental pulp stem cells. *Biomaterials* 2011;**32**:7822–30.
38. Zheng L, et al. The effect of composition of calcium phosphate composite scaffolds on the formation of tooth tissue from human dental pulp stem cells. *Biomaterials* 2011;**32**:7053–9.
39. Murray PE, About I, Lumley PJ, Franquin J-C, Remusat M, Smith AJ. Human odontoblast cell numbers after dental injury. *Journal of Dentistry* 2000;**28**:277–85.
40. Hannigan A, Lynch CD. Statistical methodology in oral and dental research: pitfalls and recommendations. *Journal of Dentistry* 2013;**41**:385–92.
41. Kanjevac T, Milovanovic M, Volarevic V, Lukic ML, Arsenijevic N, Markovic D, et al. Cytotoxic effects of glass ionomer cements on human dental pulp stem cells correlate with fluoride release. *Medicinal Chemistry* 2012;**8**:40–5.